Adaptive Backstepping and PID Control Strategy with Genetic Algorithm for PMSG by a Grid-Connected Wind Turbine

Yousra Izgheche[1], Tahar Bahi[2]
[1]Department of Electronic, Laboratory of Automatic and Signal Annaba , University Badji Mokhtar Annaba, Annaba, Algeria
[2]Department of Electrotechnic, Laboratory of Automatic and Signal Annaba , University Badji Mokhtar Annaba, Annaba, Algeria
[*]Corresponding author; Email: yousra.izgheche@univ-annaba.org.

Article Info

Article history:

Received , 29/07/2023
Revised , 10/09/2023
Accepted , 12/10/2023

Keywords:

Back-stepping control
Wind turbine
PMSG
Genetic Algorithm

ABSTRACT

In view of the importance of the trend and the need for energy transition throughout the world, and in Algeria in particular, the production of electrical energy based on renewable energy, wind energy depends essentially on wind speed, and as this is of a random nature, it therefore constitutes the problem of control to instantly extract the maximum power produced. The aim is to apply adaptive backstepping control on the turbine side and to evaluate the performance of the permanent magnet synchronous generator operating at variable speed. As well as a genetic algorithm-adjusted Integral Proportional Controller (IPC) to overcome the drawbacks of parameter sensitivity, in order to ensure efficient power management on the grid side to which the wind turbine system is connected, makes a significant contribution to improving performance, stability, reliability and research in the field of grid-connected wind power systems. The efficiency of the structure under consideration is validated using MatLab Simulink.

I. Introduction

Wind power generation is the fastest-growing form of renewable energy (RE) where the permanent magnet synchronous generator (PMSG) is the most widely used due to its advantages such as high efficiency, fast response and high power density [1] and [2]. However, this type of configuration presents many problems that complicate PMSG control, such as parametric uncertainties, variable operating conditions, non-linear dynamics and external disturbances [3]. Consequently, a lot of researchers have been talking about this problem and there are a lot of papers in the literature [4]-[9]. One of the most promising energy sources is wind power, which represents an interesting alternative, particularly for the production of electricity. The development of wind turbines has taken off in recent years, both in terms of their use around the world and in terms of their design, which has seen them evolve from small, isolated turbines to large wind farms connected to the electricity grid. On the one hand, there seems to be a need for simulation tools that can model the entire energy conversion chain and predict its performance. The overall aim is to optimize the electromechanical energy conversion of wind turbines, and to develop appropriate control. In this work, an adaptive backstepping control and a generic algorithm PID control are applied to a PMSG-based variable speed wind turbine connected to the grid via a back-to-back converter.

Based on the results of the research findings, the issues when using this control strategies in grid-connected wind turbines may include the following aspects [10]-[13]:-to ensure the system stability under variable conditions, such as wind shifts and grid load fluctuations, while maintaining optimum , the ability of adaptive backstepping control to effectively adapt to external disturbances such as wind gusts, load fluctuations, and weather changes to maintain system stability and top performances and integrating permanent magnet motor wind turbines into the power grid presents challenges in terms of synchronization, active and reactive power control, and electromagnetic interference management, and adaptive backstepping control must be able to effectively manage these aspects. In summary, the aim is to maintain the DC voltage and reactive power at their respective values, to guarantee stability, performance, adaptation to disturbances and management of system complexity.

The paper is structured as follows: Section 1 describes the conversion system, Section 2 introduces the turbine model and operation details of the permanent magnet synchronous generator, and Section 3 describes the design procedure of the proposed control strategy and describes the PI controller. We will introduce how it is applied on the network side based on Genetic Algorithm (GA). Finally, we present simulation results and conclusions. Numerical results are presented in Section 4 and Section 5, respectively.

II. Description of the conversion chain

A wind energy conversion system with a PMSG is illustrated in Figure 1. The wind energy is captured and transformed into mechanical energy by the wind turbine blades, which is then converted into electrical energy by the PMSG [14].

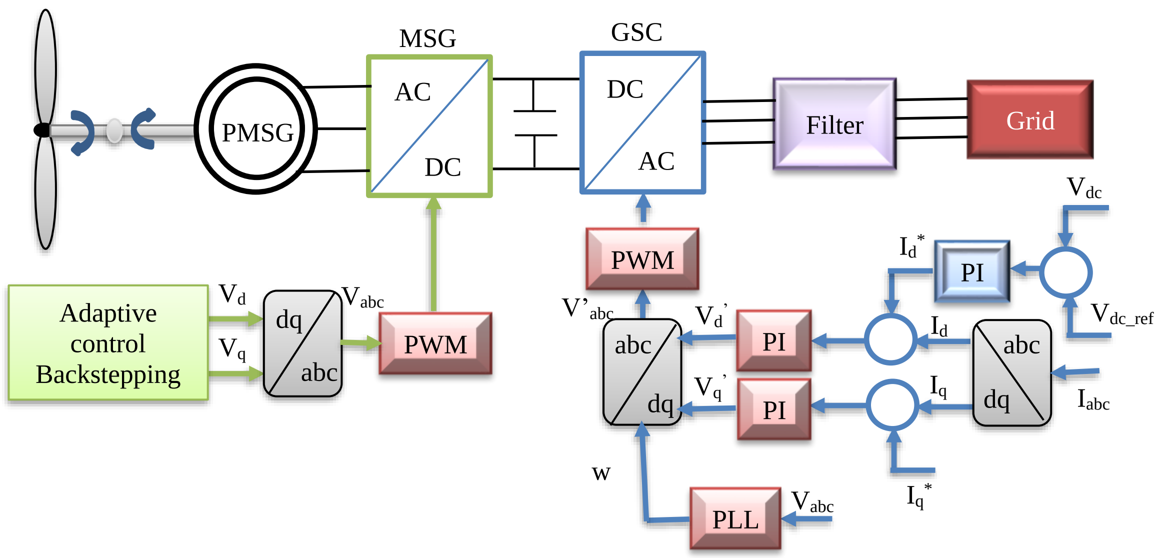

Figure 1. Schematic diagram of a generator lateral control system based on a PMSG.

An adaptive backstepping control is connected to the PMSG side to extract the maximum power required by the wind turbine depending on the wind speed. On the grid side, control is based on a proportional-integral controller (PI). In this work, in addition to classical techniques for adjusting the coefficients of the proportional term (K_p) and integral term (K_i), in particular the polar compensation technique, we also use general algorithmic approaches to: improve both performance and track maximum power points.

II.1. Modeling of Turbine

Figure 2 shows the evolution of the power coefficient as a function lamda (λ) for different values of beta (β). A maximum power coefficient of C_p = 0.45 is obtained for an optimum ratio of λ_opt = 7.07 and a fixed-pitch turbine $\beta = 0$.

The objective of PMSG-WECS is to ensure the maximum power point by adjusting the peak speed [15]. The maximum power point by adjusting the peak speed ratio is given by (1). Therefore, the rotor speed must be adjusted according to changes in wind speed. Wind speed, rotor speed must be controlled so that the turbine system operates at an optimal speed ratio lop lopt and maximum power coefficient Cp_opt: maximum power coefficient Cp (λ, β) [16] and [17].

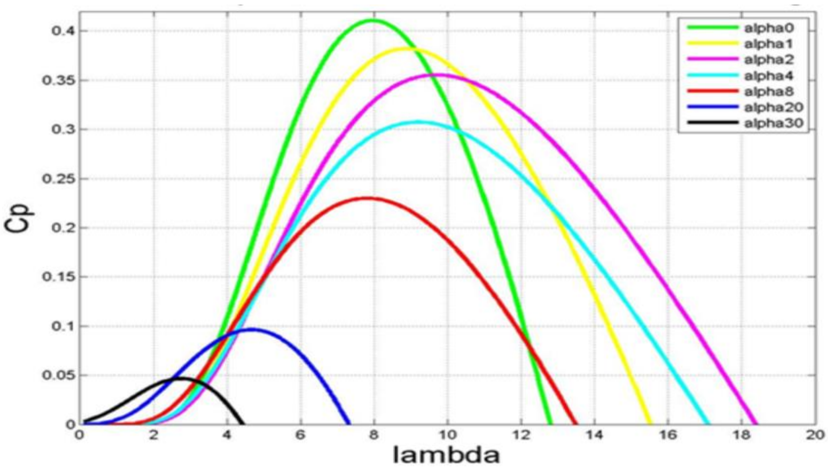

Figure 2. Power coefficient as a function of α and β.

$$P_a = \frac{1}{2}\rho\pi R^2 C_p(\lambda,\beta)V^3 \quad (1)$$

Where ρ is the air density, R is the blade radius, V is the wind speed and Cp(λ,β) de notes the power coefficient of the wind turbine, which is a function of both tip-speed-ratio l and blade pitch angle β. The mechanical torque of the turbine T_a is given [18].

$$T_a = \frac{P_a}{\omega_{rm}} = \frac{\rho\pi R^2 C_p(\lambda,\beta)V^3}{2\omega_m} \quad (2)$$

Where ω_m is the rotation speed of the wind turbine conversion system. The power coefficient (C_p) used in this study is a nonlinear function of lamda and beta, which can be expressed as follow [19]:

$$C_p(\lambda,\beta) = C_1\left(\frac{C_2}{\lambda_i} - C_3\beta - C_4\right)e^{\frac{C_5}{\lambda_i}} + C_6\lambda \quad (3)$$

With,

$$\frac{1}{\lambda_i} = \frac{1}{\lambda+0.08\beta} - \frac{0.035}{\beta^3+1} \quad (4)$$

Where the coefficients C_1 to C_6 are: C_1 = 0, 45, C_2 =116, C_3 = 0,167, C_4 = 5, C_5 = 14.34 and C_6 = 0, 00184; Tip-speed-ratio lamda is defined by:

$$\lambda = R\frac{\omega_m}{V} \quad (5)$$

II.2. Modeling of Permanent Magnet Synchronous Generator

The mathematical model of the PMSG in the rotor reference dq frame is the commonly used and it is shown as:

$$\begin{cases} V_{sd} = R_g i_d - \omega_e \varphi_{sq} + \frac{d\varphi_{sd}}{dt} \\ V_{sq} = R_g i_q - \omega_e \varphi_{sd} + \frac{d\varphi_{sq}}{dt} \end{cases} \quad (6)$$

Where, V_{gd} and V_{gq} represent the stator voltage, i_d and i_q represent the stator current, φ_{sd} and φ_{sq} represent the stator flux in the frames , R_g is the stator resistance, ω_e is the electrical rotation speed of the PMSG, defined as follows [20] and [21]:

$$\omega_e = p_r\omega_{rm} \quad (7)$$

With, p_r: is the number of pole pairs.
The stator flux expressions are as follows:

$$\begin{cases} \varphi_{sd} = L_d i_d + \varphi_f \\ \varphi_{sq} = L_q i_q \end{cases} \tag{8}$$

Where: L_d , L_q are the generator inductances on the d and q axes, φ_f is the permanent magnetic flux.
The electromagnetic torque is expressed by:

$$T_e = \frac{3}{2} p_r (\varphi_{sd} i_q - \varphi_{sq} i_d) \tag{9}$$

Substituting (8) for (6), the PMSG model in the synchronous reference frame can be expressed as follows:

$$\begin{cases} V_{gd} = R_g i_d + L_d \frac{di_d}{dt} - L_q i_q \omega_e \\ V_{gq} = R_g i_q + L_q \frac{di_q}{dt} + L_d i_d \omega_e + \omega_e \varphi_f \end{cases} \tag{10}$$

The electromagnetic torque in (9) is rewritten as follows:

$$T_e = \frac{3}{2} p_r [\varphi_f i_q + (L_d - L_q) i_q i_d] \tag{11}$$

Assuming the PMSG has equal inductances on the d and q axes (L_d / L_q), the electromagnetic torque expression in (12) can be described as follows [22]:

$$T_e = \frac{3}{2} p_r i_q \varphi f \tag{12}$$

III. Adaptative control Backstepping

For maximum power point tracking, PMSG reference commands are defined as optimal PMSG reference commands are defined as optimal mechanical angular velocity optimal mechanical angular velocity [23], $\omega_{rm\_ref} = \omega_{rm\_opt}$ and the desired d-axis current, $i_{d\_ref} = 0$.
Considering the following tracking errors:

$$\begin{cases} e_w = \omega_{rm\_opt} - \omega_{rm} \\ e_d = i_{d\_ref} - i_d \end{cases} \tag{13}$$

Next, our goal is to design controllers that guarantee that the system tracking errors in (13) to reach the neighborhoods of the origin despite uncertainties and external disturbances [24] and [25].

The PMSG control output is calculated by applying adaptive control backstepping and generating a stabilization function. The strategy based on linear feedback passivity is used to generate the current controller i_d^* is used to generate the current controller i_q^*, dq expressed in (14), represents the current reference for the controller backstepping to generate the stabilization function [26]-[28]:

First, the current tracking error vector is defined as follows:

$$e_{dq} = \begin{bmatrix} e_d \\ e_q \end{bmatrix} = \begin{bmatrix} i^*{}_d - i_d \\ i^*{}_q - i_q \end{bmatrix} \tag{14}$$

Using (13) the derivative of (14) is calculated as follows:

$$e^*_{dq} = \begin{bmatrix} e^*_d \\ e^*_q \end{bmatrix} = \begin{bmatrix} \frac{R_s}{L_d} i_d - \frac{p\omega_m L_q}{L_d} i_q - \frac{v_d}{L_d} \\ R_s^{-1} \frac{d}{dt}\left(\left(-\varphi_q^* + p\omega_m \varphi_f\right) + K_f e_{fq}\right) - \left(-\frac{R_s}{L_q} + \frac{p\omega_m L_q}{L_q} - \frac{p\omega_m \varphi_f}{L_q} - \frac{v_q}{L_q}\right) \end{bmatrix} \quad (15)$$

To design the V_{dq} controller, a Lyapunov function is defined as follows:

$$V_e = \frac{1}{2}\left(e^2{}_d - e^2{}_q\right) \quad (16)$$

The derivative of (16) gives:

$$V_e = -k_1 e^2{}_d - k_2 e^2{}_q + e_d\left(\frac{R_s}{L_d} i_d - \frac{p\omega_m L_q}{L_d} i_q - \frac{v_d}{L_d} + k_1 e_d\right) + \left(\frac{R_s}{R_s + k_f L_q} \times \left[-R_s^{-1} \varphi^{\cdot *}{}_q + p\omega_m \varphi_f \left(\frac{f_{fv}}{J R_s} + \frac{1}{L_q}\right) + i_q\left(\frac{R_s}{L_q} - \frac{(p\varphi_f)^2}{J R_s}\right) + \frac{p\varphi_f}{J R_s} T_m - \frac{V_q}{L_q} + k_2 e_q \frac{R_s + k_f L_q}{R_s}\right]\right) \quad (17)$$

After simplification, the Lyapunov function (18) becomes:

$$V_e = -k_1 e^2{}_d - k_2 e^2{}_q < 0 \quad (18)$$

Where $k_{fd} > 0$ and $k_{fq} > 0$. The overall asymptotic stability of the closed loop is guaranteed by (19) and the controller V_{dq} must be chosen as follows:

$$\begin{cases} v_d = R_s i_d - p\omega_m L_q i_q + k_1 L_d e_d \\ v_q = R_s^{-1} L_q \varphi^{\cdot *}{}_f + p\omega_m \varphi_f \left(\frac{L_q f_{fv}}{J R_s} + 1\right) + i_q\left(R_s - \frac{L_q (p\varphi_f)^2}{J R_s}\right) + \frac{L_q p \varphi_f}{J R_s} T_m + k_2 L_q e_q \frac{R_s + k_f L_q}{R_s} \end{cases} \quad (19)$$

The mathematical model of the grid- side contro (GSC) is expressed below [29].

$$\begin{bmatrix} V_{id} \\ V_{iq} \end{bmatrix} = R_f \begin{bmatrix} i_{df} \\ i_{qf} \end{bmatrix} + \begin{bmatrix} L_f i^*{}_{df} - \omega L_f i_{qf} \\ L_f i^*{}_{qf} - \omega L_f i_{df} \end{bmatrix} + \begin{bmatrix} V_{gd} \\ V_{gq} \end{bmatrix} \quad (21)$$

$$C V^*{}_{dc} = \frac{3}{2} \frac{V_{gd}}{V_{dc}} i_{df} + i_{dc} \quad (22)$$

Which: i_{df} et i_{qf} represent network currents, ω: represents the angular frequency of the network, V_{id} , V_{iq} represent inverter voltages, V_{gd} , V_{gq} represent network voltages, L_f: represents the filter inductance, R_f represents the filter resistance, V_{dc} DC voltage , C represents the DC link capacitor et i_{dc} représente le courant DC .

Active power P_g and reactive power Q_g are given as follows:

$$\begin{cases} P_g = \frac{3}{2} V_{gd} i_{qf} \\ Q_g = \frac{3}{2} V_{gd} i_{df} \end{cases} \quad (23)$$

III.1 Tuning of Regulator (PI) with genetic algorithm

The objective functions used to adjust the voltage regulator are integral square error (ISE), integral absolute error (IAE), integral time absolute error (ITAE), time squared integral error (TSIE) and time squared integral error (TSIE). All objective functions give optimal values for controller gains. However, the results obtained revealed that ITAE is the best objective function compared with the other objective functions. It delivers the best overall results [30]. Manual adjustment is the least complicated method and offers fewer possibilities for fluctuation during the adjustment procedure, but requires more time and experience [31]. GA is designed to calculate the controller gains in order to minimize the aforementioned objective functions [32].

Tuning For ITAE, GA technique is used to evaluate the controller parameters in order to Objective Function:

Minimise $f = \int_0^T t|E_v|dt$ (24)

The proportional and integral gains (K_p and K_i) produced by ITAE are 6.3 and 73.392 respectively. Using these control parameters in the Simulink model to test the circuit shown in Figure 3.

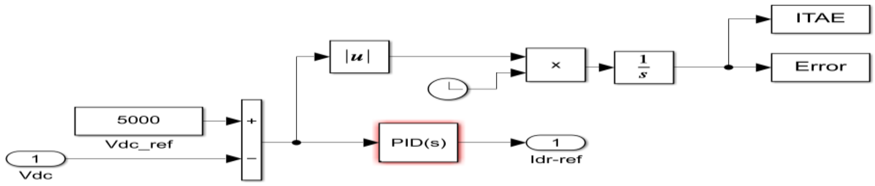

Figure 3. GA structure

IV. Results and discussion

To verify the performance validity of the Backstepping controller on the machine side and the system control on the grid side at voltage level V_{dc} a controller based on the genetic algorihme which gives good performance under a simulation model in variable wind conditions in a profile which is illustrated in Figure 4 is simulated using MatLab/Simulink.

The system parameters are shown in Table 1.

Table 1. System parameters

PMSG parameter	Value
Stator resistance (Rs)	6.25e-3 Ω
Stator inductance (Ldq)	4.229e-3 mH
Wind turbine radius (R)	55 m
Wind density (ρ)	1.22 kg/m2
Pole pairs number (p)	75
Flux linkage (ϕ f)	11.1464 Wb
Total inertia (J)	10000 kg m2
DC-link voltage (Vdc)	5000 V
DC-link capacitor (C)	0.06 F
Grid-filter resistance (Rf)	0 pu
Grid-filter inductance (Lf)	10e-3 pu

The active power is shown in Figure 5. This means that the effective power of the turbine changes according to the effective power of the generator and according to the proposed profile, increasing from 4 to 8 m/s and finally decreasing to 6 m/s t= 1 and 2 seconds. Is shown. At peak levels, you will notice that the oscillation and response times are shorter and the speed is also slower. Figure 6 shows the network reactive power (Q). The $Qref$ component is maintained at zero value to ensure unity power factor operation. Figure 7 shows the DC link voltage Vdc varying with a reference value of 5000 V, with each change in wind speed expressed as a peak change. Figure 8 shows the mechanical velocity variation of the PMSG following the reference well. You can see that the generator responds quickly to speed. Figure 9 shows the electromagnetic torque according to the standard and finally the generator current on the grid side that changes with the change in wind speed shown in Figure 10.

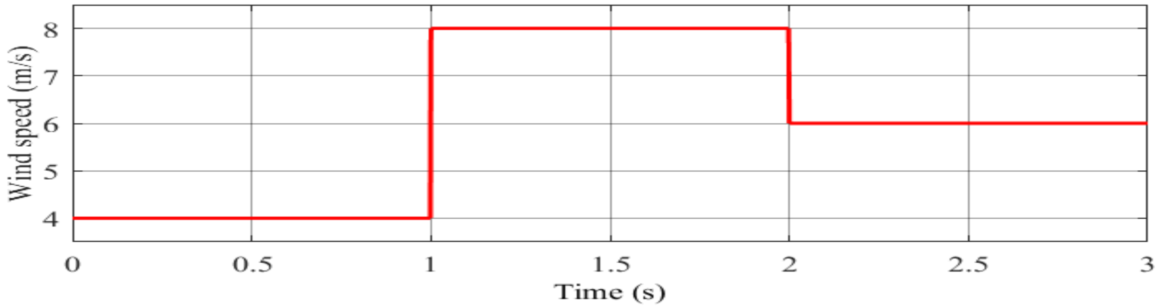

Figure 4. Profile of the wind speed.

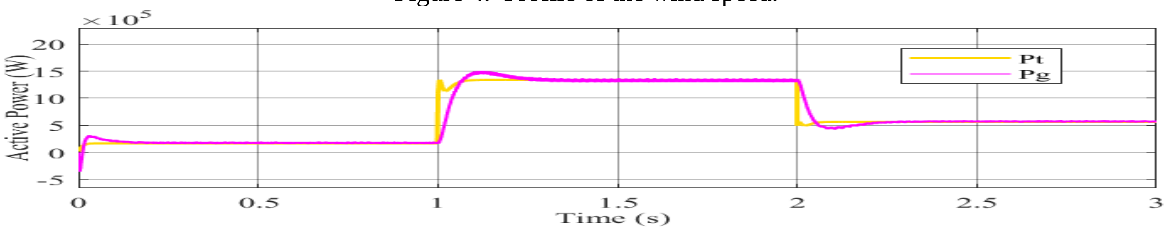

Figure 5. Active power generated.

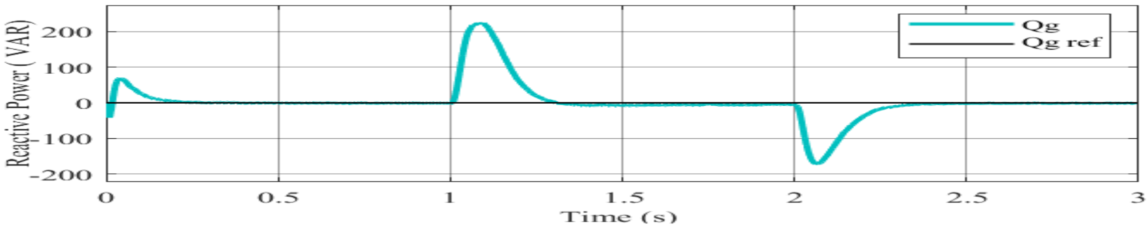

Figure 6. Reactive power generated.

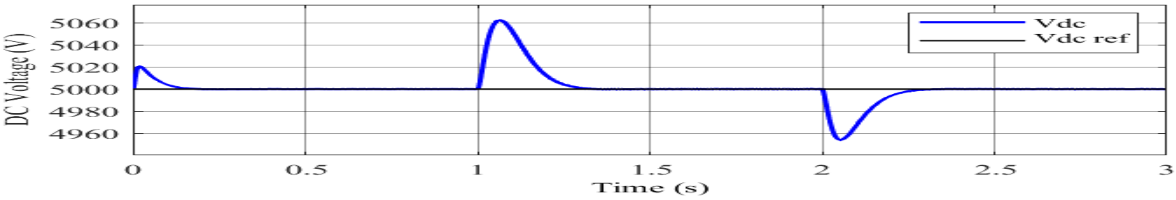

Figure 7. DC Voltage

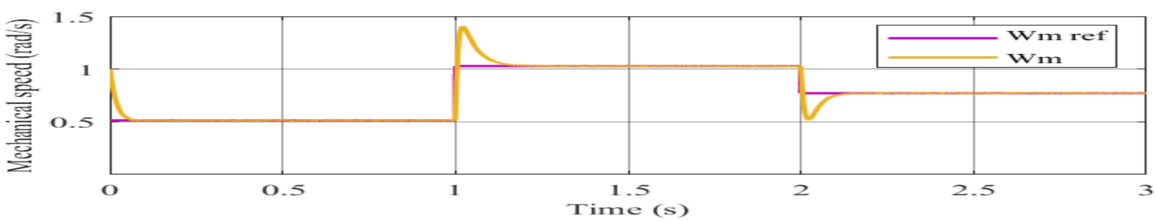

Figure 8. Mechanical speed

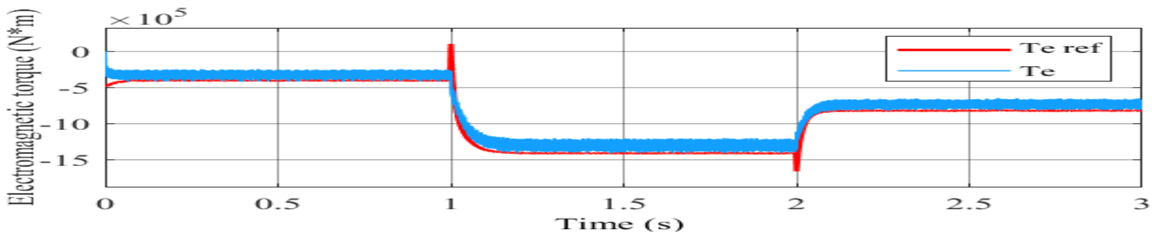

Figure 9. Electromagnetic torque

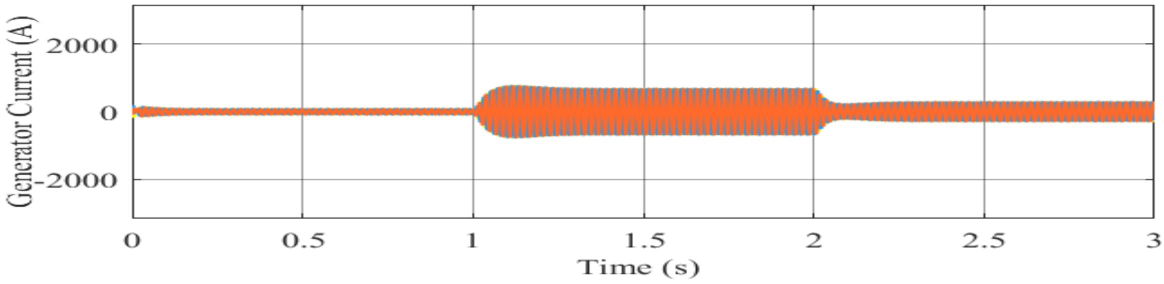

Figure 10. Generator current

V. Conclusion

The Lyapunov stability technique for optimizing WECS performance has proved promising. In fact, speed, control and setpoint tracking are assured. In addition, it can be seen that non-linear backstepping control offers better performance in different wind speeds, while robustness in the face of variations in wind profile is well assured by this control algorithm, Speed and tracking of the various variations are ensured with improved performance and the high energy efficiency and power factor around the unit attest to the efficiency of the proposed control system. So, the simulation results show that the Backstepping control strategy can improve the static and dynamic performance of a wind energy conversion system of a wind energy conversion system.

References

[1] A. Harrouz, M. Abbes, I. Colak, K. Kayisli, "Smart grid and renewable energy in Algeria". International Conference on Renewable Energy Research and Applications (ICRERA), In 2017 IEEE 6th, pp. 1166-1171. IEEE. 2017, November.

[2] A. Hatefi Einaddin, A. Sadeghi Yazdankhah and R. Kazemzadeh, "Power management in a utility connected micro-grid with multiple renewable energy sources", J. Oper. Autom. Power Eng., vol. 5, no. 1, pp. 1-9, June 2017.

[3] F. Tahiri, F. Bekraoui, F. Boussaid, I, Ouledali, O. Harrouz, "A. Direct Torque Control (DTC) SVM Predictive of a PMSM Powered by a photovoltaic source", Algerian Journal of Renewable Energy and Sustainable Development, 2019, 1(1), 1-7. https://doi.org/10.46657/ajresd.2019.1.1.1

[4] Y. Belkhier, A.Y. Achour, R.N. Shaw, " Fuzzy passivity-based voltage controller strategy of grid-connected PMSG-based wind renewable energy system", in 2020 IEEE 5th International Conference on Computing Communication and Automation (ICCCA), pp. 210–214, Greater Noida, India (2020). https://doi.org/10.1109/ICCCA49541.2020.9250838

[5] X. Wang, S. Wang, "Adaptive fuzzy robust control of PMSG with smooth inverse based deadzone compensation", Int. J. Control Autom. Syst. 14(2), 378–388 (2016).

[6] B. Yang, T. Yu, H. Shu, D. Qiu, Y. Zhang, P. Cao, L. Jiang, "Passivity-based linear feedback control of permanent magnetic synchronous generator-based wind energy conversion system: design and analysis", IET Renew. Power Gener. 12(9), 981–991 (2018).

[7] M. Nasiri, J. Milimonfared, S. H. Fathi, "Robust control of pmsg-based wind turbine under grid fault conditions," Indian J. Sci. Technol., vol. 8, no. 13, July 2015.

[8] A.R. Youssef , E.E. Mohamed , "Variable step size P&O MPPT algorithm for optimal power extraction of multi-phase PMSG based wind generation system," Int J Electr Power Energy Syst 2019;108:218–31.

[9] H. Nguyen, A.S. Al-Sumaiti, V.P. Al-Durra A, Tom Duc Do, "Optimal power tracking of PMSG based wind energy conversion systems by constrained direct control with fast convergence rates", Int J Electr Power Energy Syst, Vol. 18, june 2020.

[10] J. Wang, D. Bo, X. Ma, Y. Zhang, Z. Li, Q. Miao, " Adaptive back-stepping control for a permanent magnet synchronous generator wind energy conversion system", Int. J. Hydrogen Energy 44(5), 3240–3249 , 2019.

[11] A. Harrouz, H. Becheri, I. Colak, K. Kayisli, " Backstepping control of a separately excited DC motor", *Electrical Engineering*, *100*(3), 2018. 1393-1403.

[12] Gaidi, H. Lehouche, S. Belkacemi, S. Tahraoui, M. Loucif, W. Guenounou, "Adaptive backstepping control of wind turbine two mass model", in Proceeding of the 6th International Conference on Systems and Control, pp. 168–172, Batna, Algeria , 2017.

[13] S. Saberi, B. Rezaie, "Robust adaptive direct speed control of PMSG-based airborne wind energy system using FCS-MPC method", ISA Trans, 2022.

[14] E. Ebrahimzadeh, F. Blaabjerg, X. Wang, C.L. Bak, "Harmonic stability and resonance analysis in large PMSG-based wind power plants",I EEE Trans Sustain Energy 2018

[15] P. Falkowski, A. Sikorski, " Finite control set model predictive control for grid-connected AC–DC converters with LCL filter", IEEE Trans Ind Electron 2017; 65 (4):2844–52.

[16] B. Babaghorbani, M.T. Beheshti, H.A Talebi, "A Lyapunov-based model predictive control strategy in a permanent magnet synchronous generator wind turbine", Int J Electr Power Energy Syst 2021.

[17] F. Mazouz, S. Belkacem, I. Colak, S. Drid, Y. Harbouche, "Adaptive direct power control for double fed induction generator used in wind turbine", Int J Electr Power Energy Syst , 2020.

[18] A. Parida, D. Chatterjee, " An improved control scheme for grid connected doubly fed induction generator considering wind-solar hybrid system", Int J Electr Power Energy Syst, 2016.

[19] Y.Errami, M. Ouassaid, M. Maaroufi, "A performance comparison of a nonlinear and a linear control for grid connected PMSG wind energy conversion system", Int. J. Electr. Power Energy Syst, 2015, 68, 180–194.

[20] C.M.Hong, C.H.Chen, C.S. Tu, "Maximum power point tracking-based control algorithm for PMSG wind generation system without mechanical sensors", Energy Convers Manage, 2013, 69, 58–67.

[21] G.Dragomir, A.Şerban, G.Năstase, A.I.Brezeanu, "Wind energy in Romania: A review from 2009 to 2016. Renew. Sustain. Energy Rev. 64, 2016, 129–143 .

[22] A.Beddar, H.Bouzekri, B.Babes, H.Afghoul, "Experimental enhancement of fuzzy fractional order PI + I controller of grid connected variable speed wind energy conversion system", Energy Convers Manage. 2016, 123, 569–580.

[23] M. Benakcha, L. Benalia, A. Ammar, A. Bourek, " Wind energy conversion system based on dual stator induction generator controlled by nonlinear backstepping and pi controllers", Int. J. Syst. Assur. Eng. Manag. 2018, pp:1–11.

[24] S. R. Sanchez, M.R. Katebi, M.A. Johnson , "Tuning PID Controllers Using Subspace Identification Methods", PID Control pp: 361-388, Springer, 2005.

[25] K. Panagiotis and D. Anastasios, "Online Tuning of a PID Controller with a Fuzzy Reinforcement Learning MAS for Flow Rate Control of a Desalination Unit," Electronics, vol. 8, Feb 2019.

[26] W. M. K. A. L. Mahmud Iwan Solihin, "Objective Function Selection of GA-based PID Control Optimization for Automatic Gantry Crane", in International Conference on Computer and Communication Engineering, Kuala Lumpur, Malaysia, 2008.

[27] R.M. Linus, D. Perumal " Maximum power point tracking method using a modified perturb and observe algorithm for grid connected wind energy conversion systems", IET Renew Power Gener 2015;9(6):682e9

[28] A. Mojtaba, S.K Shokrollah, "Augmenting effectiveness of control loops of a PMSG based wind energy conversion system by a virtually adaptive PI controller", Energy 2015, pp: 610-629 Volume 91 .

[29] J. Brahmi, L. Krichen , A. Ouali , "A comparative study between three sensorless control strategies for PMSG in wind energy conversion system", Appl Energy, 2009; 86(9):1565e73.

[30] S. Ansari, Z. Jing, E.S Rajat "A Review of Stabilization Methods for DCMG with CPL, the Role of Bandwidth Limits and Droop Control", Protection and Control of Modern Power Systems, vol. 7, 2022.

[31] M. Zaliskyi, Y. Petrova, M. Asanov, and E. Bekirov, "Statistical Data Processing during Wind Generators Operation", Int. J. Electr. Electron. Eng. Telecommun,National Aviation University, Aviation Radioelectronic Complexes Department, Kyiv, Ukraine, pp. 33–38, 2019, doi: 10.18178/ijeetc.8.1.33-38.

[32] M. Abbes, "Fault-tolerant control of a PMSG-based wind turbine based on parallel interleaved converters", Turk. J. Electr. Eng. Comput. Sci., vol. 27, pp. 3219–3233, Jul. 2019, doi: 10.3906/elk-1805-149.